Learning active sensing strategies using a sensory brain–machine interface

Andrew G. Richardson[a,b,1,2], Yohannes Ghenbot[a,b,1], Xilin Liu[c], Han Hao[c], Cole Rinehart[a,b], Sam DeLuccia[a,b], Solymar Torres Maldonado[a,b], Gregory Boyek[a,b], Milin Zhang[c], Firooz Aflatouni[c], Jan Van der Spiegel[c], and Timothy H. Lucas[a,b]

[a]Department of Neurosurgery, University of Pennsylvania, Philadelphia, PA 19104; [b]Center for Neuroengineering and Therapeutics, University of Pennsylvania, Philadelphia, PA 19104; and [c]Department of Electrical and Systems Engineering, University of Pennsylvania, Philadelphia, PA 19104

Edited by Peter L. Strick, University of Pittsburgh, Pittsburgh, PA, and approved July 23, 2019 (received for review June 13, 2019)

Diverse organisms, from insects to humans, actively seek out sensory information that best informs goal-directed actions. Efficient active sensing requires congruity between sensor properties and motor strategies, as typically honed through evolution. However, it has been difficult to study whether active sensing strategies are also modified with experience. Here, we used a sensory brain–machine interface paradigm, permitting both free behavior and experimental manipulation of sensory feedback, to study learning of active sensing strategies. Rats performed a searching task in a water maze in which the only task-relevant sensory feedback was provided by intracortical microstimulation (ICMS) encoding egocentric bearing to the hidden goal location. The rats learned to use the artificial goal direction sense to find the platform with the same proficiency as natural vision. Manipulation of the acuity of the ICMS feedback revealed distinct search strategy adaptations. Using an optimization model, the different strategies were found to minimize the effort required to extract the most salient task-relevant information. The results demonstrate that animals can adjust motor strategies to match novel sensor properties for efficient goal-directed behavior.

intracortical microstimulation | water maze | rodent

Perception is an active process. Animal behaviors are replete with examples. Active sensing is not merely the exploratory movement of sensors, but instead a purposeful motor strategy to extract task-relevant sensory information, given the characteristics and constraints of the sensors (1). Common examples of active sensing include echolocation in bats (2), electrolocation in fish (3), vibrissal touch in rodents (4), and visual search in humans (5). The observed strategies are task dependent (6) and accompanied by tailored neural processing of the sensory signals (7, 8).

However, little is known about how active sensing strategies may be modified through experience (1). The acquisition of new motor skills is known to be accompanied by reciprocal plasticity in sensory and motor areas and changes in sensory perception (9). Modified strategies may also arise after neurological conditions that impair sensory or motor capabilities (10), and in subsequent use of assistive technologies. For example, such learning could be important for users of neuroprostheses that replace lesioned sensorimotor pathways with artificial ones through a brain–machine interface (BMI) (11, 12). Studying learning in this domain could reveal both the capacity for achieving new motor strategies to optimally extract sensory information and the cost functions that drive the process.

How do we effectively study learning of active sensing strategies? First, we require a closed-loop paradigm whereby task-relevant sensory information is experimentally manipulated during free behavior (13). Second, the paradigm should be parametrically controlled to show that different sensor properties result in different motor strategies (14). Finally, theoretical optimal behaviors for the different sensor properties should ideally be known to compare to the observed behaviors (14). Virtual reality paradigms provide an option to meet these objectives, as demonstrated recently in weakly electric fish (15). However, in general, virtual reality is difficult to implement in unrestrained animals (16). As an alternative, we propose that the same BMI technology developed for clinical purposes can provide an experimental platform to study learning during free behavior.

Motor BMIs, which decode neural activity to control an effector, have previously been used to study fundamental aspects of procedural learning (17–19). The closed-loop paradigm involves experimentally manipulating a learned decoder (*SI Appendix*, Fig. S1*A*) and observing how the resulting task errors, perceived naturally by the subject, drive improved performance and reorganization of the decoded neural network (20, 21). For learning active sensing strategies, we propose an analogous paradigm using sensory BMIs, which encode sensory information with direct neural stimulation (11). In this closed-loop paradigm, the encoder provides task-critical sensory information that is dependent on natural movements but that is not available to the natural senses. The encoder is then parametrically manipulated, for example, by specifying a new encoding function or brain site, and the resulting performance and behavioral strategies are assessed (*SI Appendix*, Fig. S1*B*).

Here, we used this experimental paradigm to study active sensing strategies in freely behaving rats performing open-field navigation to a hidden goal location. The closed-loop sensory BMI provided the only task-relevant information, egocentric bearing to the goal, with varying degrees of acuity. We found that the rats learned to use the artificial feedback to reliably find the goal, using distinct searching strategies that optimally identified the task-relevant information.

Significance

Our sensory experience is governed by sensor properties (e.g., eye photoreceptors) and corresponding motor strategies to sample the environment (e.g., eye movements). With injury, aging, or new task constraints, existing strategies can become incompatible with perceptual demands. Using a brain–machine interface paradigm in rats, we studied how motor strategies are adapted to new sensory inputs to accomplish a difficult searching task. We show that the strategies can be dynamically regulated through experience to optimally extract task-relevant sensory information.

Author contributions: A.G.R., F.A., J.V.d.S., and T.H.L. designed research; A.G.R., Y.G., X.L., H.H., C.R., S.D., S.T.M., G.B., and M.Z. performed research; A.G.R. and Y.G. analyzed data; and A.G.R., Y.G., and T.H.L. wrote the paper.

The authors declare no conflict of interest.

This article is a PNAS Direct Submission.

[1]A.G.R. and Y.G. contributed equally to this work.

[2]To whom correspondence may be addressed. Email: andrew.richardson@pennmedicine.upenn.edu.

This article contains supporting information online at www.pnas.org/lookup/suppl/doi:10.1073/pnas.1909953116/-/DCSupplemental.

Results

Encoding Goal Direction with ICMS. We performed a sensory BMI experiment in which task-relevant information was parametrically controlled through microstimulation of primary sensory areas. Adult rats (n = 12) were implanted chronically with a pair of cortical bipolar stimulating electrodes. During daily testing sessions, the electrodes were connected to a custom wireless neural stimulator (22) housed in a harness worn by the rat (Fig. 1*A*). The rats' task was derived from a classic behavioral paradigm, the Morris water maze (23), in which the rat was placed at the center of a pool and had to swim to a hidden, submerged platform to escape (Fig. 1*B*). Unlike the classic task, in our experiment, the platform was moved to a random location on each trial to dissociate visual cues from the platform location. The only reliable cues of platform location were the percepts evoked by swim path-dependent intracortical microstimulation (ICMS). The swim path was monitored by an overhead video camera at 12 frames/s. On each frame, the goal direction angle, θ, was computed as the deviation of the rat's current heading from the platform direction (Fig. 1*C*). A wireless transmitter updated the ICMS as a function of this angle. The encoding function was parameterized by a preferred direction (μ) and a tuning width (σ). When $\theta - \mu \leq \sigma$, the wireless stimulator delivered charge-balanced current-controlled pulses at suprathreshold intensity and 100-Hz pulse frequency. When $\theta - \mu > \sigma$, no stimulation was delivered (Fig. 1*C*). The step, rather than smooth, encoding function ensured that σ precisely defined the spatial limits of the perceived artificial feedback. Thus, σ controlled the acuity of the encoded goal direction information. The preferred direction parameter, μ, controlled the alignment of the encoded and true goal directions.

Learning with High-Acuity ICMS Feedback. Experiments began by providing a local visual cue of the platform location to establish the baseline performance. Trial performance was quantified by the ratio of the actual swim path length to the shortest path length between the start and platform locations. For the 7 rats that completed cue training (*Methods*), performance with the local visual cue was stable across the 2 to 3 sessions preceding introduction of ICMS (1-way ANOVA, $F[2,148] = 0.6$; $P = 0.549$). After the local cue was removed, the rats performed the task using only ICMS feedback. In the first pair of rats, ICMS was delivered to primary somatosensory cortex (S1) in a series of trial blocks with decreasing σ values and μ = 0°. Both rats learned to use the encoded information over the course of 100 to 200 trials, particularly for σ = 45° and 15° (Fig. 2*A*). Example pre- and postlearning trials are shown in Movies S1 and S2. The overlaid graphics in the videos indicate the conditions for stimulation on each frame (see also Fig. 2 *A*, *Top*). Stimulation was delivered when the heading vector was within the green circular sector, the area of which was defined by σ, and the orientation of which was defined by μ. In the final 30 trials of the σ = 15° block, the mean path length ratio was not significantly different from in the local visual cue block (rat Ge: $t[46] = 1.13$ [$P = 0.263$]; rat Fr: $t[62] = 0.38$ [$P = 0.700$]). Thus, when using a relatively narrow encoding function aligned with the true goal direction, the rats learned to locate the hidden platform using ICMS with the same proficiency

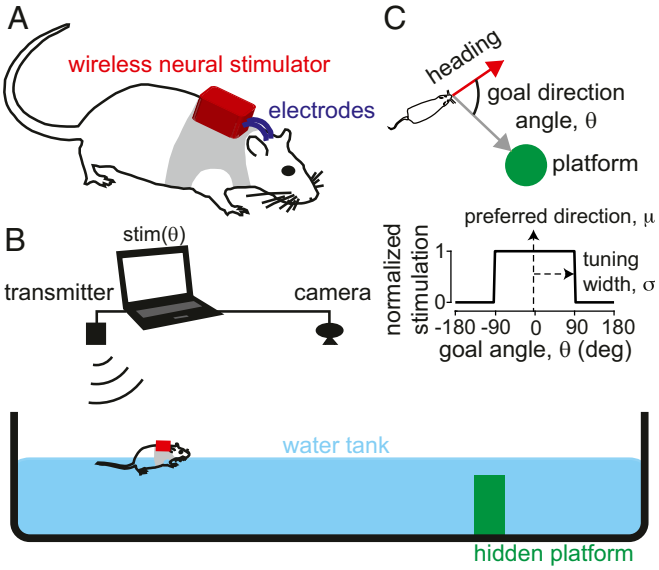

Fig. 1. Experimental paradigm. (*A*) Illustration of an instrumented subject. (*B*) Illustration of the water maze task guided by ICMS feedback. (*C*) The ICMS feedback was a step function of the goal direction angle (θ).

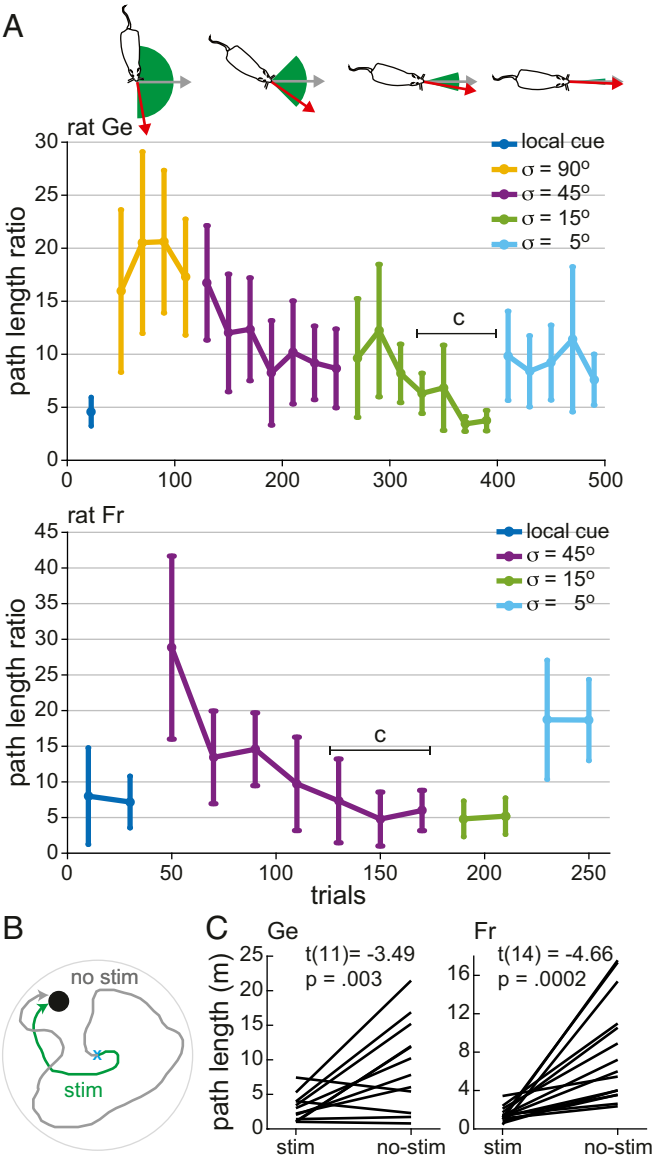

Fig. 2. Learning with high-acuity ICMS feedback. (*A*) Learning curves for rats Ge (*Top*) and Fr (*Bottom*), shown as the mean ± 95% c.i. for sequential groups of 20 trials. Illustrations at the top indicate the conditions for receiving ICMS in each trial block. ICMS was delivered when the red heading vector was within the green circular sector whose area was defined by σ. (*B*) Each catch trial (no-stim) had a platform location matched to a stimulation trial. (*C*) Results of the paired-trial analysis. Statistical tests were one-tailed. Catch trials occurred during the postlearning trial blocks indicated in *A*.

as when the platform was visible. Similar results were obtained with high-acuity ICMS feedback delivered to a different sensory area, the auditory cortex, in another rat (*SI Appendix*, Fig. S2).

Decreasing the tuning width further to $\sigma = 5°$, however, revealed an upper acuity limit. Performance became immediately worse compared with $\sigma = 15°$, and there was no improvement for up to 100 trials (Fig. 2*A*). This effect was not a trivial result of methodological limitations, such as undersampling the swim path. The video frame rate was sufficient to reliably detect each time the $\sigma = 5°$ ICMS conditions were met (Movie S3). Rather, the upper acuity limit was likely a result of perceptual limitations. Behavioral sensitivity to ICMS is known to be a function of stimulus duration, with shorter stimulus trains yielding higher detection thresholds (24, 25). Indeed, stimulus duration was approximately exponentially distributed with a mean (±SD) of 147 ± 114 ms for $\sigma = 5°$ and 417 ± 425 ms for $\sigma = 15°$. The fixed stimulus intensity was based on behavioral thresholds for 500-ms trains, thus explaining the degraded performance in $\sigma = 5°$. The existence of an acuity limit highlights an encoding tradeoff (acuity vs. detectability) in active sensing tasks, such as ours, in which the animal's movement determines ICMS duration.

To control for any performance improvements unrelated to the ICMS feedback (e.g., experience-dependent changes in general search strategy), we performed an additional analysis. After a learning criterion was met (*Methods*), occasional catch trials were introduced in which no ICMS was delivered. Platform locations on these catch trials were matched to a subset of stimulation trials, permitting a paired statistical analysis of swim path length with and without ICMS feedback (Fig. 2*B*). Although swim path length could be falsely reduced by chance encounters with the platform, the chance probability was the same for both stimulation and catch trials, as the trials were otherwise identical. Confirming use of the ICMS, the mean path length was significantly longer on catch trials (Fig. 2*C*). Additional examples of postlearning performance with high-acuity feedback, including navigating around obstacles placed in the tank, are shown in Movies S4, S5, and S6.

Learning with Low-Acuity ICMS Feedback. Next, we explored the lower limit of the acuity with which goal direction could be encoded. Specifically, we used $\sigma = 90°$, which was the lowest-acuity feedback in our paradigm, since the rats could learn to use the more specific information provided by the supplementary σ and μ angles for $\sigma > 90°$. For example, encoding functions with parameters $\mu = 0°$, $\sigma = 135°$, and $\mu = 180°$, $\sigma = 45°$ would both specify the goal direction to within 45° and were thus equivalent in terms of their information content.

Rat Ge failed to show much improvement using $\sigma = 90°$ for 85 trials (Fig. 2*A*). However, we found that when given more trials, 3 other rats learned the task. For example, rat Sa showed a performance improvement over the course of 123 trials (Fig. 3*A*), although the final performance (last 30 trials) was worse than the baseline visual cue performance ($t[46] = -2.11$; $P = 0.040$). Interestingly, when the directionality of the ICMS was reversed such that stimulation occurred when moving away from the platform ($\mu = 180°$), rat Sa reached a performance plateau statistically indistinguishable from the visual cue baseline ($t[46] = -0.96$; $P = 0.345$). First, this result demonstrates reversal learning of our encoding paradigm, whereby after first learning one ICMS contingency, the animal had the capacity to remap the appropriate behavioral response to a new ICMS contingency (26). Second, it shows that even when ICMS encoded the platform direction with very low acuity, the rat learned to locate the platform with the same proficiency as with a visual cue. The same was true of 2 other rats (Sn and Ro), as summarized by the paired statistical analysis comparing trials with and without ICMS after learning (Fig. 3*B*). Similar results were obtained with the low-acuity paradigm in a simpler task in which the platform could be in 1 of only 4 known locations. In this 4-location task, we found that the rats prioritized use of the stimulation over the relatively simple alternative of visiting each location in turn (*SI Appendix*, Fig. S3).

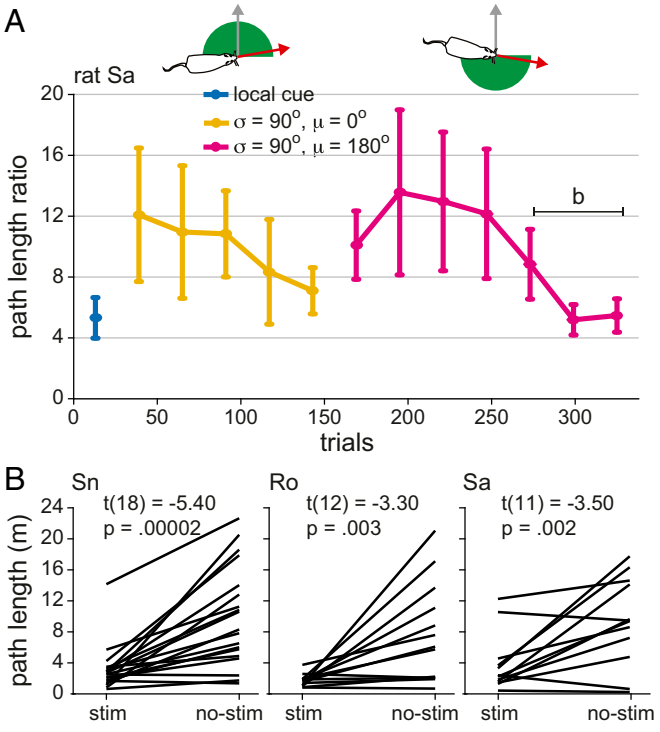

Fig. 3. Learning with low-acuity ICMS feedback. (*A*) Task performance (mean ± 95% c.i. for sequential groups of 25 trials) of rat Sa with a local visual cue (dark blue), with stimulation when swimming toward the platform (yellow), and with stimulation when swimming away from the platform (pink). Illustrations at the top indicate the conditions for receiving neural stimulation in each trial block. (*B*) Paired statistical analysis of the performance with and without ICMS ($\sigma = 90°$, $\mu = 180°$) for rat Sa and 2 other rats.

ICMS Transitions Provided Optimal Goal Localization Signal. The preceding performance analyses indicate that the rats learned to use the ICMS feedback in both high- and low-acuity conditions. However, they do not reveal how the feedback was used or whether behavioral strategies varied between artificial sensory conditions, which is a key requirement of active sensing (14). Theoretically, the ambiguity in the ICMS feedback could be largely resolved by focusing on the stimulation transitions. For example, for the encoding parameters $\sigma = 90°$ and $\mu = 180°$, at the ICMS off-to-on transition, the platform is on the line oriented exactly 90° from the current heading (Fig. 4*A*). More generally, for any σ and μ, the platform direction is $\varphi = \left|arg\left(e^{i[\sigma-\mu]}\right)\right|$ from the instantaneous heading at the ICMS transition. The only remaining ambiguity, due to our encoding of the unsigned goal-direction angle, is whether to turn to the left or right by φ at the transition. Note that the ICMS transition was the maximum slope, or edge, of the encoding function. Previous work has shown that use of an edge of a sensory signal (e.g., odor trail) is optimal for spatial localization (27).

Search Strategies Were Dependent on Encoding Parameters. Noise in the rats' estimate of their heading and delays in perception of the ICMS transition would hamper use of the optimal strategy described here. Their swimming momentum would further prevent the immediate turn required for its execution. Improved knowledge of the platform direction might be attained iteratively by accumulating evidence over multiple ICMS transitions. Furthermore, conserving momentum by a looping swim path at the transition might aid execution. We observed both of these behaviors in the actual swim paths. For example, in the trial shown in Fig. 4*B* ($\sigma = 90°$, $\mu = 180°$), a first ICMS train occurred during the initial circular swim path in the middle of the tank. The lines at

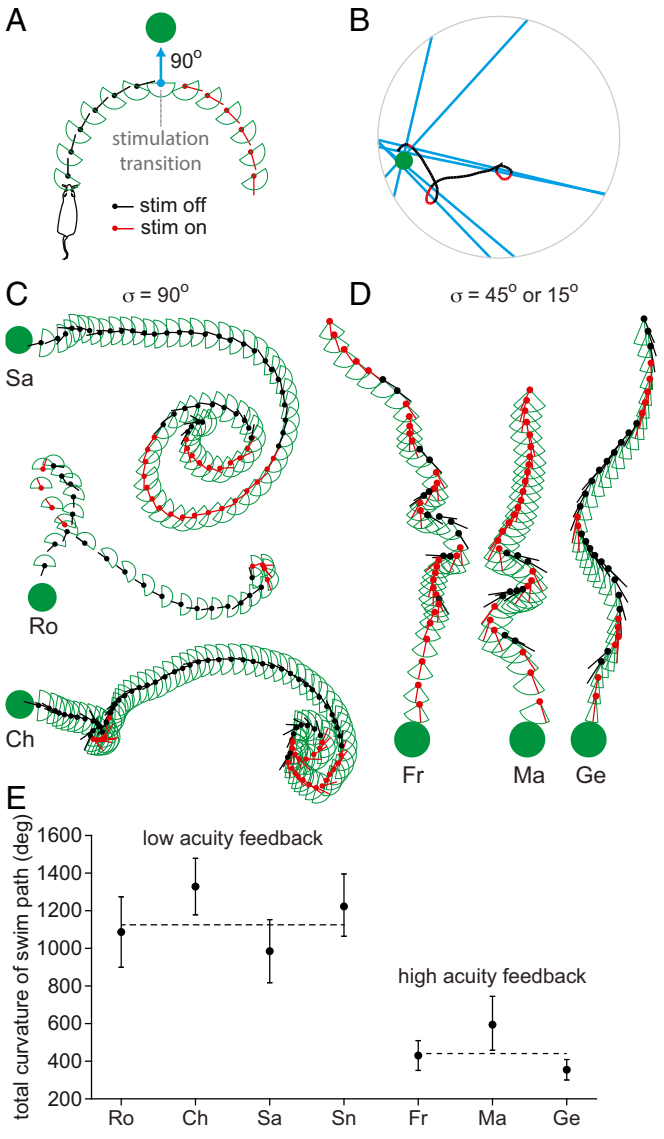

Fig. 4. Strategies for using the ICMS feedback. (*A*) Illustration of how a ICMS transition (off-to-on) could be used to identify the goal-direction vector (blue arrow) for σ = 90°, μ = 180°. (*B*) Actual trial (rat Ro, σ = 90°, μ = 180°) demonstrating the goal direction lines (blue) at σ° from the heading at each ICMS (red) transition. (*C*) Typical examples of actual swim paths for σ = 90° for 3 rats. (*D*) Typical examples of actual swim paths for σ = 45° (rats Fr, Ma) or σ = 15° (rat Ge). (*E*) Total curvature of the swim path (mean ± 95% c.i.) for postlearning trials of each rat.

angle $\varphi = 90°$ from the instantaneous swim path at the ICMS off-to-on and on-to-off points are shown in blue. With this initial information, the rat then swam generally toward the platform, but with a clear deviation from the true direction. Then, a second ICMS train occurred, prompting a corrective loop leading closer to the platform. Finally, the rat overshoots, receives a third ICMS train, and makes a final turn to reach the platform. A similar strategy was observed across all the rats that learned the σ = 90° condition (e.g., Movies S7 and S8). In particular, the rats swam in a spiral or circular pattern in the middle of the tank to efficiently gather initial ICMS feedback, followed by a swim toward the platform with a tight corrective loop if ICMS was encountered again (Fig. 4*C*).

In contrast, in the σ = 45° and 15° conditions, the rats adopted a very different strategy. The swim paths almost entirely lacked any tight spiraling or looping. Instead, often a zigzagging strategy was used in which side-to-side movements generated ICMS transitions, presumably to better define the goal direction (Fig. 4*D*). A similar strategy has been observed in rats following a wide odor trail (28). To quantify the difference in looping versus zigzagging swim trajectories, we computed the total curvature of the swim path (i.e., the sum of the rat's yaw rotation between each pair of consecutive frames) for each postlearning trial. The mean total curvature was significantly higher in the 4 rats that learned to use low-acuity feedback than in the 3 rats that learned to use high-acuity feedback (Fig. 4*E*; $t[5] = 5.74$; $P = 0.0022$). Importantly, there was no mean performance difference, quantified by path length ratio, between these same groups ($t[5] = 0.002$; $P = 0.9984$). Thus, with equivalent performance, the characteristics of the encoded sensory information caused distinct motor strategies to be learned.

Search Strategies Minimized Effort Needed to Identify ICMS Transitions. Finally, we asked why these different strategies might be appropriate for the encoded directional sense. As just described, the encoding function edges, or ICMS transitions, provided the most information for goal localization. From the point of view of mechanics, looping and zigzagging might minimize the torque needed to rotate in the water to find the edges of wide and narrow encoding functions, respectively. To explore this hypothesis, we considered a simple model of yaw rotation dynamics: $\tau = Id^2\theta/dt^2 + bd\theta/dt$, where $\tau(t)$ was the control torque, $\theta(t)$ was the heading (goal-direction) angle, I was the yaw axis moment of inertia, and b was the coefficient of frictional resistance (or drag) in water. Using Pontryagin's minimum principle, we derived optimal solutions to control the heading trajectory from an initial condition of $\theta(0) = 0°$, to $\theta(t_1) = \sigma$ (first edge), and then to $\theta(T) = -\sigma$ or $2\pi - \sigma$ (second edge, zigzagging or looping; *SI Appendix*). We also left as a free parameter the angular speed, ρ, at $t = t_1$ and $t = T$. The optimal time of first edge interception, $t_1{}^*$, optimal heading, $\theta^*(t)$, and optimal control torque, $\tau^*(t)$, were determined separately for the zigzagging and looping terminal constraints. We then compared the total effort (i.e., integrated squared torque) used by zigzagging and looping to determine which strategy was optimal over a range of model parameters (*SI Appendix*).

Two examples are shown in Fig. 5*A*. Using estimates of I and b based on the rats' body morphology, we found that it was more efficient to zigzag than to loop when σ = 45°, in agreement with the rats' learned behavior (Fig. 5 *A*, *Left*). For the same parameters, when the encoding function was widened to σ = 75°, it was optimal to loop rather than zigzag (Fig. 5 *A*, *Right*). In general, the optimal strategy for a given σ was dependent on the ratio b/I and ρ (Fig. 5*B*). Over the range of parameters tested, it was always optimal to loop at σ = 90°. For σ < 90°, zigzagging became optimal at slower angular speeds or if drag relative to inertia became large. At σ < 50°, it was always optimal to zigzag (Fig. 5*B*). Thus, this simple mathematical model and hypothesized cost function produced results that were in general agreement with the observed search strategies used by the rats. Furthermore, the model predicts that we should observe looping behaviors at 50° < σ < 90°, provided the angular speeds used by the rats are sufficiently high.

Discussion

The majority of sensory BMI studies have focused on the detection and discrimination of ICMS in the absence of information-seeking movement (i.e., passive sensing) (11, 24, 25, 29). The relatively few active sensing BMI studies to date have used searching tasks, where the goal is recognizable (e.g., by external reward), but its location is found only through interpretation of ICMS feedback or by random search. In these searching tasks, 2 types of feedback have been tested: goal contact and goal direction. In the contact paradigm, ICMS is delivered when a natural or neuroprosthetic effector spatially overlaps the goal (30–32). This feedback is analogous to tactile signals arising from contact with an object. Therefore, the paradigm is informative to

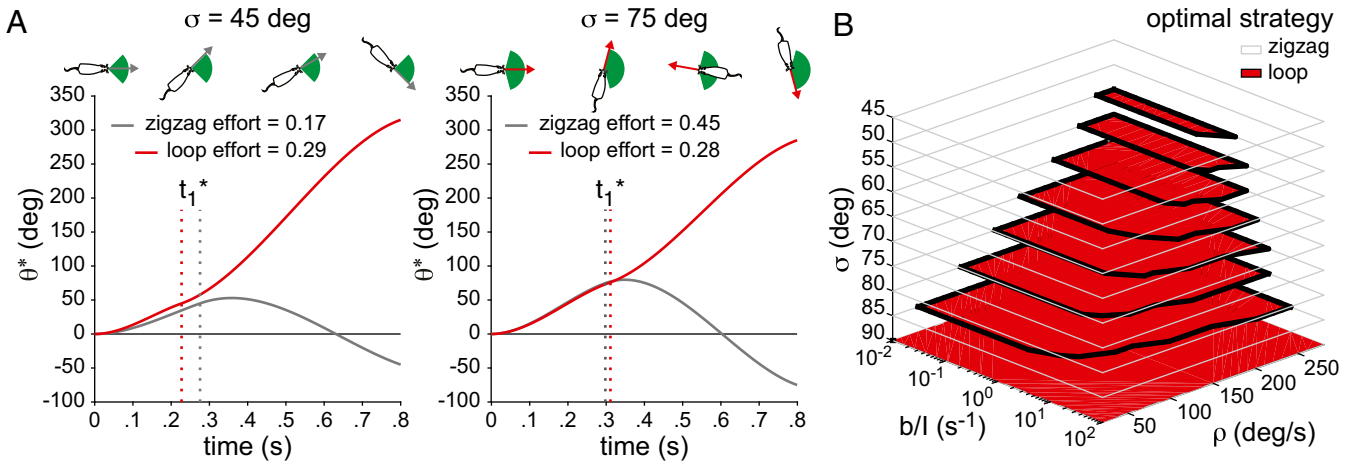

Fig. 5. Modeling optimal search strategies. (*A*) Optimal heading trajectory, θ*(t), to identify edges of an encoding function with width of σ = 45° (*Left*) or σ = 75° (*Right*), using a zigzagging strategy (gray) and a looping strategy (red). Model parameters were $I = 6.5 \times 10^{-4}$ N·m·s^2, $b = 1.5 \times 10^{-5}$ N·m·s, $\rho = 200$°/s, and T = 0.8 s. The optimal time to first edge (t_1*) and integrated squared torque (effort) are indicated for each strategy. Illustrations of the model rat's heading using the minimum effort strategy are indicated at the top for 4 points along the trajectory. (*B*) Model predictions of the optimal strategy over a range of parameters and T = 0.7 s.

an artificial sense of touch for neuroprostheses. However, for the study of active sensing, the paradigm is limited, since the motor strategy to search for the goal is independent of ICMS until the point at which it is encountered. In the direction paradigm, ICMS provides feedback about the goal direction, which is noncontact spatial information analogous to natural vision or audition rather than touch, and which is naturally encoded in entorhinal-hippocampal circuits (33, 34). This paradigm affords the subject an opportunity to tailor their motor behavior to the ICMS feedback properties to efficiently search for the goal. Prior work has shown that rats can learn to discriminate between 4 potential goal locations on the basis of ICMS delivered when their heading coincides with the direction of the true goal location (35). Several variations on this result were subsequently reported (26, 36, 37).

Our sensory BMI experiment also used a searching task with goal direction feedback. However, several features distinguish our study from prior ones. First, we parametrically varied the encoding function to directly explore whether and how searching strategies varied with feedback properties. Specifically, we tested the full range of the parameter specifying acuity of the artificial sense. Performance and goal direction acuity had a U-shaped relationship, which we interpreted as resulting from a decrease in ICMS detectability at higher acuities. This tradeoff might be circumvented by mimicking natural sensory adaptation (38), with intensity starting high enough for short bouts of ICMS to be detected and gradually decreasing such that longer episodes remain perceivable while minimizing charge injection. Importantly, we also observed different learned active sensing strategies: looping for low-acuity feedback and zigzagging for high-acuity feedback. Prior studies investigated reversal learning by changing the encoding function, but only at the level of performance (26, 36). Second, we identified an optimal strategy as a function of the encoding parameters, which involved precise turning at ICMS transitions. The swim paths indicated that ICMS transitions were indeed exploited. Our model indicated that the learned strategies were optimal for encountering these transitions. Third, we used a continuous-location searching task, implemented in a water maze to provide intrinsic goal-seeking motivation (23). The task was significantly more challenging, requiring many more trials to learn, than prior discrete-location tasks. Impressively, the rats learned to use ICMS to locate the randomly located hidden platform with the same proficiency as natural vision.

Together, these features establish sensory BMI as a platform for studying learning of active sensing strategies. Much of the active sensing literature is devoted to elucidating the elegant solutions, refined through evolution, that model organisms use to enhance sensory information through movement (39, 40). Solutions are often hard-coded in the body plan and movement abilities of the animal, distribution of sensory receptors, and tuning of primary sensory neurons. However, changes in neural response properties, neural functional connectivity, and attentional sampling could allow active sensing routines to be shaped through experience (41). An important line of inquiry is to investigate how active sensing strategies are dynamically regulated or adapted to changes in an organism's sensorimotor apparatus or ecological niche (13). Sensory BMI, compared with virtual reality, is more compatible with studying learning during free behavior. A potential disadvantage is the nonethological nature of the stimuli. Thus, the sensory BMI method is particularly well suited to studying active sensing adaptations to pathological or unnatural sensorimotor contingencies, such as occurs with neurological injury and neuroprosthetic treatments. As exemplified by our work, such studies can reveal the animal's learning capacity in this domain, the explicit relationship between sensor properties and sensing strategies, and how the strategies compare to known optimal alternatives.

Methods

Surgery. The following procedures were approved by the University of Pennsylvania Institutional Animal Care and Use Committee. Sprague-Dawley rats (n = 12; male; initial weight 250–275 g) were purchased from Charles River Laboratories. Before surgery, the rats were habituated to handling for approximately 1 wk. Then, an aseptic surgical procedure was performed to implant a concentric bipolar stimulating electrode (MS308, Plastics One), with 150-μm inner electrode diameter and 1-mm interelectrode distance, into a target cortical area. The rats were given preemptive analgesia (buprenorphine SR, 1.2 mg/kg) and anesthetized with an i.p. injection of ketamine (60 mg/kg) and dexmedetomidine (0.25 mg/kg). Once placed in a stereotaxic frame, a 2-mm-diameter craniectomy was performed and the electrode was slowly advanced into either S1 or A1 (coordinates in *SI Appendix*, Fig. S4). Dental acrylic was applied to form a permanent headcap around the electrode and skull screws. The rats were given 7 d after surgery to recover before training resumed.

Training. After recovery from surgery, the rats were reintroduced to handling and habituated to wearing a harness to which a wireless neural stimulator was attached (Fig. 1*A*). Then, they performed a visually guided search task for 3 to 7 daily sessions in a Morris water maze (23). The Morris water maze consisted of a 2-m circular metal tank with a black interior, filled with water of ambient temperature (18–22 °C) to a depth of about 25 cm. The water was made opaque with black tempura paint to hide a 10-cm circular

acrylic platform submerged by 2 cm. On the visually guided task, a white ruler protruding 15 cm above the water was attached to the platform to provide a local visual cue of its location. On each trial, the platform was moved to a random location. Each trial began by placing the rat within a body length of the center of the tank (13.7 ± 2.3 cm from center on average across all trials and rats) and at a relatively consistent orientation (27.8° SD). The rat then swam to find the platform to escape the maze. Training concluded when the rat consistently appeared to be actively looking for the local visual cue and reaching the platform without anxious or inattentive behaviors such as clinging to or following the walls of the tank (thigmotaxis). Performance on the final 20–30 trials of the visually guided task was used to provide a baseline to which learning on the stimulation-based task was compared. All animals that completed training as described were included in the experiment ($n = 7$). Four rats were excluded due to repeated signs of stress (e.g., excess vocalization) and thigmotaxis during training that did not ameliorate over time. Per our protocol, these animals were removed from the study. An additional rat was excluded after its chronic implant detached from the head.

Experiment. After training, the local visual cue was replaced with ICMS that encoded the rats' egocentric bearing to the platform. The objective of the experiment was to see whether and how the rats learned to use this artificially encoded information. The encoding paradigm required a closed-loop system to update ICMS parameters in real-time, based on the swim path (Fig. 1*B*). The custom closed-loop system was described previously (22). Briefly, a video camera with a 1080p image sensor was placed above the center of the Morris water maze to monitor the rat's swim path at 12 frames/s. A computer program (MATLAB) acquired each video frame, identified the rat's heading relative to the platform, and computed ICMS parameters based on the encoding function specified by the experimenter (Fig. 1*C*). The rat's heading was determined by identifying, on each frame, a red landmark on the wearable stimulator corresponding to the position of the rat's upper back, and computing the orientation of the vector between the identified positions on every pair of consecutive frames. On each video frame, the updated ICMS parameters were sent wirelessly to the neural stimulator, using a 2.4-GHz transceiver.

The wearable stimulator ($20 \times 25 \times 15$ mm, 15 g) delivered bipolar, biphasic, current-controlled pulses with programmable pulse width, pulse amplitude, and pulse frequency. For these experiments, pulse width and frequency were fixed at 0.2 ms/phase and 100 Hz, respectively. Pulse amplitude, determined at the beginning of each session, was set at the threshold for a behavioral response to 500-ms pulse trains. Current amplitude was increased until the experimenter detected a clear response (e.g., turning the head contralaterally or twitching or scratching the whisker pad) to 2 consecutive pulse trains (42). The range of pulse amplitudes used was 15 to 75 μA. The stimulator was battery powered, encased in waterproof rubber latex, and attached to the harness via cable-tie fasteners. The stimulator transmitted back to the acquisition computer on each frame the measured voltage on the electrodes. This allowed us to track the electrode impedance throughout each trial, and to exclude trials in which large impedance changes occurred, typically due to water infiltration or loosening of the electrode connector. These events occurred on less than 3% of trials.

Experiments consisted of a series of multisession trial blocks in which different encoding functions were tested. Testing conditions for each rat are listed in *SI Appendix*, Table S1. To assess learning, the effect size (Hedges' g statistic) was computed between the path length ratio distributions of the local visual cue trials and ICMS trials in nonoverlapping 20 trial blocks. Two consecutive ICMS trial blocks with a $|g| < 0.5$ was used as the learning criterion. Catch trials, in which no ICMS was delivered, were randomly interleaved with ICMS trials in the postlearning periods to further assess reliance on the ICMS feedback. Through the use of catch trials, each rat served as its own control. At the conclusion of the study, the electrodes were localized to the target cortical areas using histology (*SI Appendix*).

ACKNOWLEDGMENTS. We thank Pauline Weigand, Adam Engelson, Amy Danoff, Kathleen Propert, and Andrew Cucchiara for assistance in this research. Y.G. was supported by the National Center for Advancing Translational Sciences under award no. TL1TR001880.

1. T. J. Prescott, M. E. Diamond, A. M. Wing, Active touch sensing. *Philos. Trans. R. Soc. Lond. B Biol. Sci.* **366**, 2989–2995 (2011).
2. Y. Yovel, B. Falk, C. F. Moss, N. Ulanovsky, Active control of acoustic field-of-view in a biosonar system. *PLoS Biol.* **9**, e1001150 (2011).
3. G. von der Emde, Active electrolocation of objects in weakly electric fish. *J. Exp. Biol.* **202**, 1205–1215 (1999).
4. J. B. Schroeder, J. T. Ritt, Selection of head and whisker coordination strategies during goal-oriented active touch. *J. Neurophysiol.* **115**, 1797–1809 (2016).
5. J. Najemnik, W. S. Geisler, Optimal eye movement strategies in visual search. *Nature* **434**, 387–391 (2005).
6. V. C. Paulun, A. C. Schutz, M. M. Michel, W. S. Geisler, K. R. Gegenfurtner, Visual search under scotopic lighting conditions. *Vision Res.* **113**, 155–168 (2015).
7. L. Busse *et al*., Sensation during active behaviors. *J. Neurosci.* **37**, 10826–10834 (2017).
8. D. N. Rushton, J. C. Rothwell, M. D. Craggs, Gating of somatosensory evoked potentials during different kinds of movement in man. *Brain* **104**, 465–491 (1981).
9. D. J. Ostry, P. L. Gribble, Sensory plasticity in human motor learning. *Trends Neurosci.* **39**, 114–123 (2016).
10. G. Veneri, A. Federico, A. Rufa, Evaluating the influence of motor control on selective attention through a stochastic model: The paradigm of motor control dysfunction in cerebellar patient. *BioMed Res. Int.* **2014**, 162423 (2014).
11. S. N. Flesher *et al*., Intracortical microstimulation of human somatosensory cortex. *Sci. Transl. Med.* **8**, 361ra141 (2016).
12. L. R. Hochberg *et al*., Reach and grasp by people with tetraplegia using a neurally controlled robotic arm. *Nature* **485**, 372–375 (2012).
13. V. Hofmann, M. J. Chacron, Active sensing: Constancy requires change. *Curr. Biol.* **28**, R1391–R1394 (2018).
14. S. C. Yang, D. M. Wolpert, M. Lengyel, Theoretical perspectives on active sensing. *Curr. Opin. Behav. Sci.* **11**, 100–108 (2018).
15. D. Biswas *et al*. Closed-loop control of active sensing movements regulates sensory slip. *Curr. Biol.* **28**, 4029–4036.e4 (2018).
16. D. A. Dombeck, M. B. Reiser, Real neuroscience in virtual worlds. *Curr. Opin. Neurobiol.* **22**, 3–10 (2012).
17. M. D. Golub, S. M. Chase, A. P. Batista, B. M. Yu, Brain-computer interfaces for dissecting cognitive processes underlying sensorimotor control. *Curr. Opin. Neurobiol.* **37**, 53–58 (2016).
18. K. A. Moxon, G. Foffani, Brain-machine interfaces beyond neuroprosthetics. *Neuron* **86**, 55–67 (2015).
19. J. D. Wander, R. P. Rao, Brain-computer interfaces: A powerful tool for scientific inquiry. *Curr. Opin. Neurobiol.* **25**, 70–75 (2014).
20. B. Jarosiewicz *et al*., Functional network reorganization during learning in a brain-computer interface paradigm. *Proc. Natl. Acad. Sci. U.S.A.* **105**, 19486–19491 (2008).
21. P. T. Sadtler *et al*., Neural constraints on learning. *Nature* **512**, 423–426 (2014).
22. X. Liu *et al*., "A wireless neuroprosthetic for augmenting perception through modulated electrical stimulation of somatosensory cortex" in *2017 IEEE International Symposium on Circuits and Systems (ISCAS)* (IEEE, 2017), pp. 1–4.
23. C. V. Vorhees, M. T. Williams, Morris water maze: Procedures for assessing spatial and related forms of learning and memory. *Nat. Protoc.* **1**, 848–858 (2006).
24. G. Y. Fridman, H. T. Blair, A. P. Blaisdell, J. W. Judy, Perceived intensity of somatosensory cortical electrical stimulation. *Exp. Brain Res.* **203**, 499–515 (2010).
25. S. Kim *et al*., Behavioral assessment of sensitivity to intracortical microstimulation of primate somatosensory cortex. *Proc. Natl. Acad. Sci. U.S.A.* **112**, 15202–15207 (2015).
26. K. Hartmann *et al*., Embedding a panoramic representation of infrared light in the adult rat somatosensory cortex through a sensory neuroprosthesis. *J. Neurosci.* **36**, 2406–2424 (2016).
27. Y. Yovel, B. Falk, C. F. Moss, N. Ulanovsky, Optimal localization by pointing off axis. *Science* **327**, 701–704 (2010).
28. A. G. Khan, M. Sarangi, U. S. Bhalla, Rats track odour trails accurately using a multilayered strategy with near-optimal sampling. *Nat. Commun.* **3**, 703 (2012).
29. R. Romo, A. Hernández, A. Zainos, E. Salinas, Somatosensory discrimination based on cortical microstimulation. *Nature* **392**, 387–390 (1998).
30. C. Klaes *et al*., A cognitive neuroprosthetic that uses cortical stimulation for somatosensory feedback. *J. Neural Eng.* **11**, 056024 (2014).
31. J. E. O'Doherty *et al*., Active tactile exploration using a brain-machine-brain interface. *Nature* **479**, 228–231 (2011).
32. S. Venkatraman, J. M. Carmena, Active sensing of target location encoded by cortical microstimulation. *IEEE Trans. Neural. Syst. Rehabil. Eng.* **19**, 317–324 (2011).
33. A. Sarel, A. Finkelstein, L. Las, N. Ulanovsky, Vectorial representation of spatial goals in the hippocampus of bats. *Science* **355**, 176–180 (2017).
34. C. Wang *et al*., Egocentric coding of external items in the lateral entorhinal cortex. *Science* **362**, 945–949 (2018).
35. E. E. Thomson, R. Carra, M. A. Nicolelis, Perceiving invisible light through a somatosensory cortical prosthesis. *Nat. Commun.* **4**, 1482 (2013).
36. H. Norimoto, Y. Ikegaya, Visual cortical prosthesis with a geomagnetic compass restores spatial navigation in blind rats. *Curr. Biol.* **25**, 1091–1095 (2015).
37. E. E. Thomson *et al*., Cortical neuroprosthesis merges visible and invisible light without impairing native sensory function. *eNeuro* **4**, ENEURO.0262-17.2017 (2017).
38. S. Chung, X. Li, S. B. Nelson, Short-term depression at thalamocortical synapses contributes to rapid adaptation of cortical sensory responses in vivo. *Neuron* **34**, 437–446 (2002).
39. V. Hofmann *et al*., Sensory flow shaped by active sensing: Sensorimotor strategies in electric fish. *J. Exp. Biol.* **216**, 2487–2500 (2013).
40. M. E. Nelson, M. A. MacIver, Sensory acquisition in active sensing systems. *J. Comp. Physiol. A Neuroethol. Sens. Neural Behav. Physiol.* **192**, 573–586 (2006).
41. C. E. Schroeder, D. A. Wilson, T. Radman, H. Scharfman, P. Lakatos, Dynamics of active sensing and perceptual selection. *Curr. Opin. Neurobiol.* **20**, 172–176 (2010).
42. E. K. Brunton, E. B. Yan, K. L. Gillespie-Jones, A. Lowery, R. Rajan, "Chronic thresholds for evoking perceptual responses in the rat sensory cortex" in *2015 7th International IEEE/EMBS Conference on Neural Engineering (NER)* (IEEE, 2015), pp. 502–505.